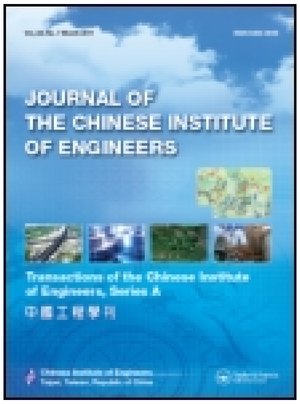

Journal of the Chinese Institute of Engineers
Publication details, including instructions for authors and subscription information:
http://www.tandfonline.com/loi/tcie20

Tip-off effect analysis of a vehicle moving along an inclined guideway by considering dynamic interactions

Sheng-Nan Chou [a], Fu-Ping Cheng [a] & Chiung-Shiann Huang [a]
[a] Department of Civil Engineering, National Chiao Tung University, Hsinchu, Taiwan 300, ROC
Published online: 10 Oct 2012.

Journal of the Chinese Institute of Engineers, 2013
Vol. 36, No. 2, 164–172, http://dx.doi.org/10.1080/02533839.2012.727597

Tip-off effect analysis of a vehicle moving along an inclined guideway by considering dynamic interactions

Sheng-Nan Chou*, Fu-Ping Cheng and Chiung-Shiann Huang

Department of Civil Engineering, National Chiao Tung University, Hsinchu, Taiwan 300, ROC

(*Received 8 June 2011; final version received 10 September 2011*)

This study investigates the tip-off effect responses of an accelerated vehicle by considering the dynamic interaction between the vehicle and its guideway system. The launch system is considered as an inclined simply supported uniform elastic beam, whereas the vehicle is regarded as a rigid beam moving along the elastic beam under the action of a predetermined thrust force. A technique for tip-off effect analysis that takes into account the dynamic interactions is developed. Equations governing the interaction between the rigid beam and its guideway are derived by taking into account the influences of the inertia force, Coriolis force, and centrifugal force, on the basis of the Euler–Bernoulli beam theory. A comparison of the tip-off analysis results of the elastic and rigid guideway models indicates that the dynamic response obtained for the elastic guideway model was 20% greater than that obtained for the rigid guideway model. The simulation results of the influences of several parameters by tip-off effect analysis can provide information that is valuable when designing vehicle launch systems.

Keywords: tip-off effect; dynamic interaction; moving mass; moving load

1. Introduction

Many studies have focused on the transverse vibration of beams under the influence of moving loads or moving masses (Michaltsos *et al*. 1996, Fryba 1999, Michaltsos 2002, Lin and Weng 2004, Wu 2005, Dehestani *et al*. 2009). Vehicle–bridge interaction dynamics have been extensively studied for application to high-speed railways (Xia *et al*. 2003, Xia and Zhang 2005, Yang and Wu 2005). In particular, Yang *et al*. (1997) investigated the vibration of simple beams during the passage of high-speed trains. In the field of control engineering, generally, a vehicle (e.g., missiles) and its guideway are together considered to constitute a rigid body for the tip-off analysis to be carried out (Yao and Zhang 1998). Two aspects of this assumption require to be investigated in detail. First, the mass of a launched vehicle is considerably larger than that of its guideway. The model of a rigid guideway considers neither the inertia force of a heavy mass moving across a light guideway nor the dynamic interaction between the vehicle and its guideway. Second, the initial movement of the vehicle at the end of the take-off phase will affect the flight control of the vehicle. Therefore, in order to obtain a more precise analytical result and minimize the dynamic response of the vehicle during take-off from the viewpoint of safety, the dynamic interaction between the vehicle and its guideway must be studied in detail.

We modeled the vehicle as a rigid beam, and the launcher guideway as an inclined elastic simply supported beam. The vehicle is connected to the guideway with two contact points by means of an interface, which is regarded as a rigid connection so that the dynamic responses of these two points are forced to be equal during the process of the vehicle take-off. To resolve this dynamic problem with moving coupling systems, this article employs a modal superposition approach to convert the governing equations into a set of generalized systems associated with the moving equations of the vehicle. In this study, the present results provide available information for a launched vehicle running over an inclined guideway in its launch operating phase.

2. *Guideway mathematical formulation*

A typical straight guideway vehicle launcher system is shown schematically in Figure 1. We separate the vehicle and guideway as two free bodies in Figure 2. This study can be extended to any kind of application of prescribed thrust force. We assumed the typical thrust–time curve, as shown in Figure 3 in this study,

*Corresponding author. Email: snchou48@gmail.com

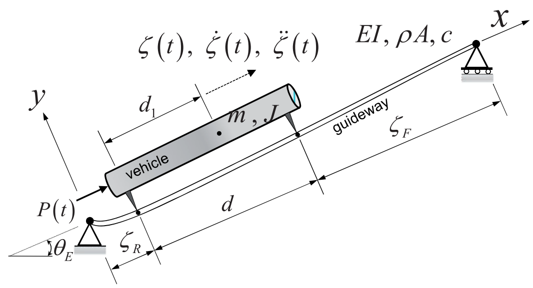

Figure 1. A typical straight guideway vehicle launcher model.

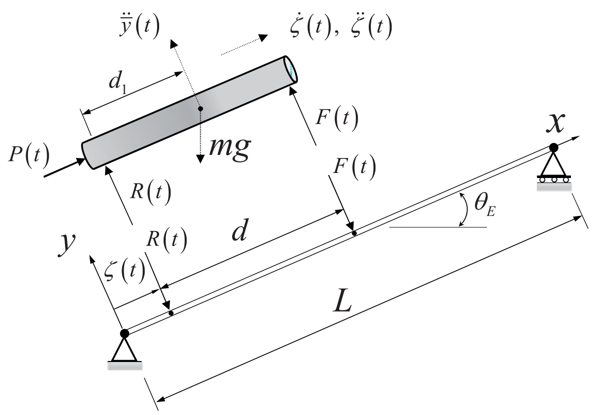

Figure 2. A vehicle and its guideway free-body diagram.

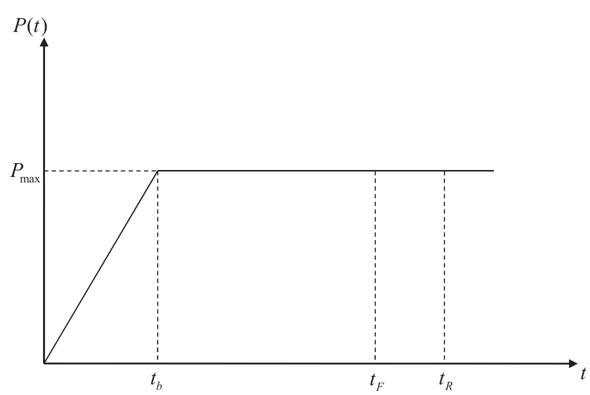

Figure 3. A typical thrust–time curve.

where t_b is the thrust build-up time, $P_{\max}$ the value of $P(t)$ after t_b, t_F the time of vehicle front shoe losing contact, and t_R the time of vehicle rear shoe losing contact. We refer to t_R as the tip-off time. During t_F and t_R the vehicle tip-off effect will happen.

2.1. *The position history of a moving vehicle*

The motion of the vehicle can be divided into two phases. They are the two shoes contact and the tip-off phases. According to the typical thrust–time curve as well as the design parameters of the vehicle and its guideway, we can obtain the position of rear shoe $\zeta(t)$ shown as Figure 2, t_F and t_R to determine which phase the vehicle motion belongs to. The values of $\zeta(t)$ and $\dot{\zeta}(t)$ can be obtained from Newton's mechanics, t_F and t_R can be given in the following formulations:

$$t_F = t_b + \frac{m}{(P_{\max} - mg\sin\theta_E)} \times \left[\sqrt{\dot{\zeta}(t_b)^2 + \frac{2}{m}[\zeta_F - \zeta(t_b)][(P_{\max} - mg\sin\theta_E)]} - \dot{\zeta}(t_b)\right], \quad (1)$$

$$t_R = t_b + \frac{m}{(P_{\max} - mg\sin\theta_E)} \times \left[\sqrt{\dot{\zeta}(t_b)^2 + \frac{2}{m}[\zeta_F - \zeta(t_b) + d][(P_{\max} - mg\sin\theta_E)]} - \dot{\zeta}(t_b)\right], \quad (2)$$

where ζ_R is the distance from rear shoe of vehicle to left end of guideway at $t = 0$, and ζ_F the distance from front shoe of vehicle to right end of guideway at $t = 0$.

2.2. *Two shoes contact phase*

The vibration of the guideway is modeled by an Euler–Bernoulli simply supported beam with viscous damping and subjected to initial conditions as well as specific boundary conditions. We assumed the symbols F and R are the moving loads of the contact points. Based on the deflection theory of small deformations for beam, the governing equation of vertical vibration can be written as the following partial differential equation:

$$EI\frac{\partial^4 u(x,t)}{\partial x^4} + \rho A\frac{\partial^2 u(x,t)}{\partial t^2} + c\frac{\partial u(x,t)}{\partial t} = R\delta(x,\zeta) + F\delta(x,\zeta + d), \quad (3)$$

where $u(x,t)$ is the transverse displacement of the guideway at coordinate x at time t; EI the constant flexural rigidity of the guideway; ρA the mass per unit length of the guideway; c the damping coefficient per unit length; $\delta(\cdot)$ the *Dirac delta function*; and $R\delta(x,\zeta) + F\delta(x,\zeta+d)$ an external force acting on the guideway because of the motion of the vehicle in the two shoes contact phase.

Based on the aforementioned assumptions and the relationship of geometry in Figure 4, we can obtain $\bar{y} = \frac{d_1}{d}y_F + \frac{(d-d_1)}{d}y_R$ and $\bar{\theta} = \frac{y_F - y_R}{d}$. Accordingly, the equations of motion for the vehicle can be written as

$$m\ddot{\bar{y}} = -R - F + mg\cos\theta_E, \quad (4)$$

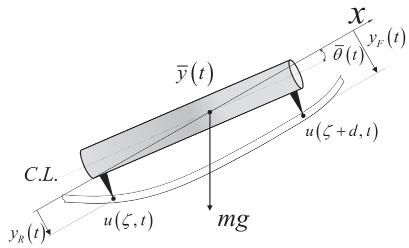

Figure 4. A typical displacement of guideway during the vehicle moving along the guideway.

$$J\ddot{\bar{\theta}} = d_1 R - (d - d_1)F. \tag{5}$$

The equations of the contact load between the vehicle and its guideway are derived by taking into account the effects of the inertia force, Coriolis force, and centrifugal force of the moving vehicle. These equations can be expressed as follows:

$$R = m[\bar{g}r_2 - J_3(\ddot{y}_R + 2\dot{y}'_R\dot{\zeta} + y''_R\dot{\zeta}^2) + J_1(\ddot{y}_F + 2\dot{y}'_F\dot{\zeta} + y''_F\dot{\zeta}^2)], \tag{6}$$

$$F = m[\bar{g}r_1 + J_1(\ddot{y}_R + 2\dot{y}'_R\dot{\zeta} + y''_R\dot{\zeta}^2) - J_2(\ddot{y}_F + 2\dot{y}'_F\dot{\zeta} + y''_F\dot{\zeta}^2)], \tag{7}$$

where the overhead dot $(\cdot)$ and prime $(')$ denote the differentiation with respect to time t and coordinate x, respectively; $\dot{\zeta}$ the velocity of the moving vehicle in the local x-direction; y_R and y_F the displacements of the two contact points in the y-direction of the guideway when the vehicle is moving along a deformed guideway; $(\ddot{y}_R, \ddot{y}_F)$, $(2\dot{y}'_R\dot{\zeta}^2, 2\dot{y}'_F\dot{\zeta})$, and $(y''_R\dot{\zeta}^2, y''_F\dot{\zeta}^2)$ the acceleration of the inertia force, Coriolis force, and centrifugal force at the shoes of rear and front contact points, respectively; and the constants r_1, r_2, J_1, J_2, J_3, and $\bar{g}$ are defined as follows:

$$r_1 = \frac{d_1}{d}, \quad r_2 = \frac{d - d_1}{d}, \quad \bar{g} = g\cos\theta_E,$$
$$J_1 = \frac{J}{md^2} - r_1 r_2, \quad J_2 = \frac{J}{md^2} + r_1^2, \quad J_3 = \frac{J}{md^2} + r_2^2, \tag{8}$$

where m represents the mass of the vehicle, J the principal transverse moment of inertia of the vehicle, d the length between shoes of the vehicle, d_1 the length from rear shoe to center of gravity of the vehicle, θ_E the inclined angle of guideway, and g the gravitational acceleration.

In order to obtain the approximate solution of the coupled system equations, the transverse displacement of the guideway $u(x,t)$ can be expressed as the supposition of the normal mode as in the following equation:

$$u(x,t) = \sum_{i=1}^{\infty} \phi_i(x) Y_i(t); \quad 0 \le t \le t_F, \tag{9}$$

where $\phi_i(x)$ denotes the ith mode of the guideway that satisfies the boundary conditions. $Y_i(t)$ is the generalized coordinate corresponding to the i mode. Particularly, we used the modes of natural vibrations of a simply supported homogeneous beam:

$$\phi_i(x) = \sin\left(\frac{i\pi x}{L}\right). \tag{10}$$

Substituting Equations (6), (7), (9), and (10) into Equation (3), multiplying both sides of the equation by $\phi_n(x)$ and integrating with respect to x over the length L of the beam, we obtained an expression of the form:

$$\ddot{Y}_i(t) + \rho_M \sum_{j=1}^{N} \Phi_{mij} \ddot{Y}_j(t) + 2\xi_i\omega_i \dot{Y}_i(t) + \rho_M \sum_{j=1}^{N} \Phi_{cij} \dot{Y}_j(t)$$
$$+ \omega_i^2 Y_i(t) + \rho_M \sum_{j=1}^{N} \Phi_{kij} Y_j(t) = Q_i, \tag{11}$$

where $i = 1 \ldots N$, $\rho_M = 2m/\rho AL$, $\rho_F = 2m\bar{g}/\rho AL$, ω_i =circular frequency of the ith vibration of the guideway, and Q_i, Φ_{mij}, Φ_{cij}, Φ_{kij} can be given as follows:

$$Q_i = \rho_F\left\{r_2 \sin\left(\frac{i\pi\zeta}{L}\right) + r_1 \sin\left[\frac{i\pi(\zeta+d)}{L}\right]\right\}, \tag{12}$$

$$\Phi_{mij} = \left\{J_3 \sin\left(\frac{j\pi\zeta}{L}\right) - J_1 \sin\left[\frac{j\pi(\zeta+d)}{L}\right]\right\} \times \sin\left(\frac{i\pi\zeta}{L}\right) - \left\{J_1 \sin\left(\frac{j\pi\zeta}{L}\right) - J_2 \sin\left[\frac{j\pi(\zeta+d)}{L}\right]\right\} \sin\left[\frac{i\pi(\zeta+d)}{L}\right]. \tag{13}$$

$$\Phi_{cij} = \frac{2j\pi\dot{\zeta}}{L}\left\{J_3 \cos\left(\frac{j\pi\zeta}{L}\right) - J_1 \cos\left[\frac{j\pi(\zeta+d)}{L}\right]\right\} \times \sin\left(\frac{i\pi\zeta}{L}\right) - \frac{2j\pi\dot{\zeta}}{L}\left\{J_1 \cos\left(\frac{j\pi\zeta}{L}\right) - J_2 \cos\left[\frac{j\pi(\zeta+d)}{L}\right]\right\} \sin\left[\frac{i\pi(\zeta+d)}{L}\right]. \tag{14}$$

$$\Phi_{kij} = \left(\frac{j\pi\dot{\zeta}}{L}\right)^2\left\{-J_3 \sin\left(\frac{j\pi\zeta}{L}\right) + J_1 \sin\left[\frac{j\pi(\zeta+d)}{L}\right]\right\} \times \sin\left(\frac{i\pi\zeta}{L}\right) + \left(\frac{j\pi\dot{\zeta}}{L}\right)^2\left\{J_1 \sin\left(\frac{j\pi\zeta}{L}\right) - J_2 \sin\left[\frac{j\pi(\zeta+d)}{L}\right]\right\} \sin\left[\frac{i\pi(\zeta+d)}{L}\right]. \tag{15}$$

where $i = 1, \ldots, N$ and $j = 1, \ldots, N$.

Since the system is initially at rest, the guideway's initial velocity and acceleration are zero, so the initial conditions are $\ddot{Y}_i(0) = 0$, $\dot{Y}_i(0) = 0$, $\dot{\zeta} = 0$, $\Phi_{cij} = 0$, and $\Phi_{kij} = 0$, and its initial generalized coordinates $Y_i(0)$ due to the static loads of vehicle mass can be expressed as:

$$Y_i(0) = \frac{\rho_F}{\omega_i^2}\left\{r_2 \sin\left(\frac{i\pi\zeta_R}{L}\right) + r_1 \sin\left[\frac{i\pi(\zeta_R + d)}{L}\right]\right\}. \quad (16)$$

2.3. *Tip-off phase*

When the front shoe loses contact with the guideway, F reduces to zero at the tip-off phase. The vehicle and guideway are considered to be two free bodies, as shown in Figure 5.

The transverse vibrations in the guideway can be expressed as follows:

$$EI\frac{\partial^4 u(x,t)}{\partial x^4} + \rho A\frac{\partial^2 u(x,t)}{\partial t^2} + c\frac{\partial u(x,t)}{\partial t} = R^*\delta(x,\zeta), \quad (17)$$

$$R^* = m\left(\frac{J_1 + r_1 r_2}{J_2}\right)\left[\bar{g} - (\ddot{y}_R + 2\dot{y}'_R\dot{\zeta} + y''_R\dot{\zeta}^2)^*\right]. \quad (18)$$

For the tip-off phase, we set

$$u(x,t) = \sum_{i=1}^{\infty}\phi_i(x)Y_i^*(t); \qquad t_F < t \leq t_R. \quad (19)$$

Hence, using a procedure similar to that described above, we obtain

$$\ddot{Y}_i^*(t) + \rho_M^*\sum_{j=1}^{N}\Phi_{mij}^*\ddot{Y}_j^*(t) + 2\xi_i\omega_i\dot{Y}_i^*(t) + \rho_M^*\sum_{j=1}^{N}\Phi_{cij}^*\dot{Y}_j^*(t) + \omega_i^2 Y_i^*(t) + \rho_M^*\sum_{j=1}^{N}\Phi_{kij}^*Y_j^*(t) = Q_i^*, \quad (20)$$

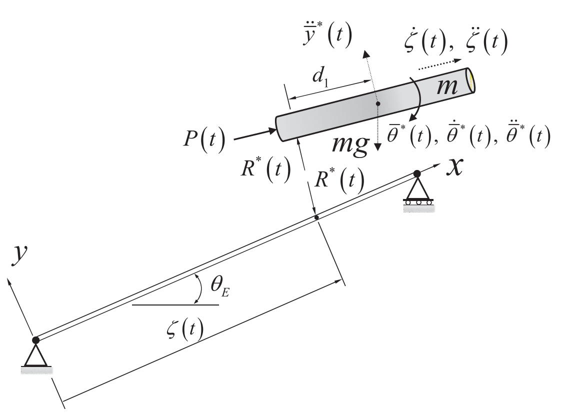

Figure 5. Free-body diagrams of vehicle in tip-off phase.

where $i = 1 \ldots N$, $\rho_M^* = 2m(J_1 + r_1 r_2)/(\rho A L J_2)$, $\rho_F^* = 2m\bar{g}(J_1 + r_1 r_2)/(\rho A L J_2)$, and Q_i^*, Φ_{mij}^*, Φ_{cij}^*, Φ_{kij}^* can be given as follows:

$$Q_i^* = \rho_F^* \sin\left(\frac{i\pi\zeta}{L}\right), \quad (21)$$

$$\Phi_{mij}^* = \sin\left(\frac{j\pi\zeta}{L}\right)\sin\left(\frac{i\pi\zeta}{L}\right), \quad (22)$$

$$\Phi_{cij}^* = \frac{2j\pi\dot{\zeta}}{L}\cos\left(\frac{j\pi\zeta}{L}\right)\sin\left(\frac{i\pi\zeta}{L}\right), \quad (23)$$

$$\Phi_{kij}^* = -\left(\frac{j\pi\dot{\zeta}}{L}\right)^2\sin\left(\frac{j\pi\zeta}{L}\right)\sin\left(\frac{i\pi\zeta}{L}\right), \quad (24)$$

where $i = 1 \ldots N$ and $j = 1 \ldots N$.

These equations are subject to the continuity conditions $Y_i^*(0) = Y_i(t_F)$ and $\dot{Y}_i^*(0) = \dot{Y}_i(t_F)$, i.e., the displacements and velocities of the guideway are continuous.

3. Calculation of dynamic response of guideway

It should be emphasized that Equations (11) and (20) represent a set of coupled second-order differential equations. Equations (9) and (18) can be rewritten in the form of a matrix, as follows:

$$\boldsymbol{M}\ddot{\boldsymbol{Y}} + \boldsymbol{C}\dot{\boldsymbol{Y}} + \boldsymbol{K}\boldsymbol{Y} = \boldsymbol{Q} \quad (25)$$

Here, $\boldsymbol{Y}$ is a generalized coordinate; $\dot{\boldsymbol{Y}}$ a generalized velocity; $\ddot{\boldsymbol{Y}}$ a generalized acceleration; $\boldsymbol{Q}$ a generalized force; $\boldsymbol{M}$ a generalized mass matrix; $\boldsymbol{C}$ a generalized damping matrix; and $\boldsymbol{K}$ a generalized stiffness matrix. The differential-algebraic system technique was used to obtain numerical solutions of these equations. Equation (25) was transformed into a system of first-order differential equations in the state space form by taking time as an additional variable.

4. Formulation of dynamic response of vehicle tip-off

If the dynamic responses of the guideway, $u(x,t)$, $u(x+d,t)$, $\dot{u}(x,t)$, and $\dot{u}(x+d,t)$, for any time t corresponding to the two phases are determined, the dynamic responses of the guideway at any position x can be obtained. Using these results, we can formulate the dynamic responses of vehicle tip-off as follows:

- For $t = 0$, the system is initially at rest:

For $u(x, 0)$, the position displacement of the guideway, x, is given by

$$u(x,0) = \sum_{i=1}^{N} \sin\left(\frac{i\pi x}{L}\right) \frac{2m\bar{g}}{\rho A L \omega_i^2} \left\{ r_2 \sin\left(\frac{i\pi \zeta_R}{L}\right) + r_1 \sin\left[\frac{i\pi(\zeta_R + d)}{L}\right] \right\}. \tag{26}$$

For $\bar{y}(0)$, the displacement of the vehicle's center of gravity is given by

$$\begin{aligned}\bar{y}(0) &= r_1 u(\zeta_R + d, 0) + r_2 u(\zeta_R, 0) \\ &= \sum_{i=1}^{N} \frac{2m\bar{g}}{\rho A L \omega_i^2} \left\{ r_2 \sin\left(\frac{i\pi \zeta_R}{L}\right) + r_1 \sin\left[\frac{i\pi(\zeta_R + d)}{L}\right] \right\}.\end{aligned} \tag{27}$$

For $\bar{\theta}(0)$, the pitch angle of the vehicle is given as

$$\begin{aligned}\bar{\theta}(0) &= \frac{1}{d}[u(\zeta_R + d, 0) - u(\zeta_R, 0)] \\ &= \sum_{i=1}^{N} \frac{2m\bar{g}}{\rho A L \omega_i^2} \left\{ \sin\left[\frac{i\pi(\zeta_R + d)}{L}\right] - \sin\left(\frac{i\pi \zeta_R}{L}\right) \right\} \\ &\quad \times \left\{ r_2 \sin\left(\frac{i\pi \zeta_R}{L}\right) + r_1 \sin\left[\frac{i\pi(\zeta_R + d)}{L}\right] \right\}.\end{aligned} \tag{28}$$

- For $0 < t \le t_F$:

For $u(\zeta, t)$, the position displacement of the guideway, ζ, at time t is given by

$$u(\zeta, t) = \sum_{i=1}^{N} \phi_i(\zeta) Y_i(t) = \sum_{i=1}^{N} \sin\left(\frac{i\pi\zeta}{L}\right) Y_i(t). \tag{29}$$

For $\bar{y}(t)$, the displacement of the vehicle's center of gravity at time t is given by

$$\begin{aligned}\bar{y}(t) &= r_1 u(\zeta + d, t) + r_2 u(\zeta, t) \\ &= \sum_{i=1}^{N} \left\{ r_1 \sin\left[\frac{i\pi(\zeta + d)}{L}\right] + r_2 \sin\left(\frac{i\pi\zeta}{L}\right) \right\} Y_i(t).\end{aligned} \tag{30}$$

For $\dot{\bar{y}}(t)$, the velocity of the vehicle's center of gravity at time t is given by

$$\begin{aligned}\dot{\bar{y}}(t) &= r_1 \dot{u}(\zeta + d, t) + r_2 \dot{u}(\zeta, t) \\ &= \sum_{i=1}^{N} \left\{ r_1 \sin\left[\frac{i\pi(\zeta + d)}{L}\right] + r_2 \sin\left(\frac{i\pi\zeta}{L}\right) \right\} \dot{Y}_i(t).\end{aligned} \tag{31}$$

For $\bar{\theta}(t)$, the pitch angle of the vehicle at time t is given by

$$\begin{aligned}\bar{\theta}(t) &= \frac{1}{d}[u(\zeta + d, t) - u(\zeta, t)] \\ &= \frac{1}{d}\sum_{i=1}^{N} \left\{ \sin\left[\frac{i\pi(\zeta + d)}{L}\right] - \sin\left(\frac{i\pi\zeta}{L}\right) \right\} Y_i(t).\end{aligned} \tag{32}$$

For $\dot{\bar{\theta}}(t)$, the pitch rate of the vehicle at time t is given by

$$\begin{aligned}\dot{\bar{\theta}}(t) &= \frac{1}{d}[\dot{u}(\zeta + d, t) - \dot{u}(\zeta, t)] \\ &= \frac{1}{d}\sum_{i=1}^{N} \left\{ \sin\left[\frac{i\pi(\zeta + d)}{L}\right] - \sin\left(\frac{i\pi\zeta}{L}\right) \right\} \dot{Y}_i(t).\end{aligned} \tag{33}$$

- For $t_F < t \le t_R$:

During the vehicle tip-off phase, the front shoe loses contact with the guideway, while the rear shoe of the vehicle continues to move along the guideway. The vehicle is subjected to the thrust force, inertia force, Coriolis force, and centrifugal force. The vehicle rotates with respect to its rear shoe. The free-body diagram of the vehicle shows that its center of gravity is acted upon by the gravitational acceleration, and simultaneously, its rear shoe is acted upon by the acceleration $(\ddot{y}_R + 2\dot{y}'_R\dot{\zeta} + y''_R\dot{\zeta}^2)^*$ in the y-direction. The equations of equilibrium for the vehicle body are

$$\begin{aligned}\sum F_y &= m\left[\bar{g} - \left(\ddot{y}_R + 2\dot{y}'_R\dot{\zeta} + y''_R\dot{\zeta}^2\right)^*\right] = ma_y, \\ \sum M_o &= I_o\ddot{\bar{\theta}}^* = d_1 m a_y.\end{aligned} \tag{34}$$

Hence, the rotational acceleration of the vehicle with respect to its rear shoe is defined as follows:

$$\begin{aligned}\ddot{\bar{\theta}}^*(t) = \frac{r_1}{J_2 d}\Bigg\{ \bar{g} - \sum_{i=1}^{N} \Bigg[\ddot{Y}_i^*(t)\sin\left(\frac{i\pi\zeta}{L}\right) \\ + \frac{2i\pi\dot{\zeta}}{L}\cos\left(\frac{i\pi\zeta}{L}\right)\dot{Y}_i^*(t) - \left(\frac{i\pi\dot{\zeta}}{L}\right)^2 \sin\left(\frac{i\pi\zeta}{L}\right) Y_i^*(t) \Bigg]\Bigg\}.\end{aligned} \tag{35}$$

From the continuity of the displacements and velocities of the guideway in the two phases, we can obtain the continuity conditions $Y_i^*(0) = Y_i(t_F)$ and $\dot{Y}_i^*(0) = \dot{Y}_i(t_F)$.

For $\bar{\theta}^*(t)$, the pitch angle of the vehicle at time t is given by

$$\bar{\theta}^*(t) = \bar{\theta}(t_F) + (t - t_F)\dot{\bar{\theta}}(t_F) + \frac{1}{2}\ddot{\bar{\theta}}^*(t)(t - t_F)^2. \tag{36}$$

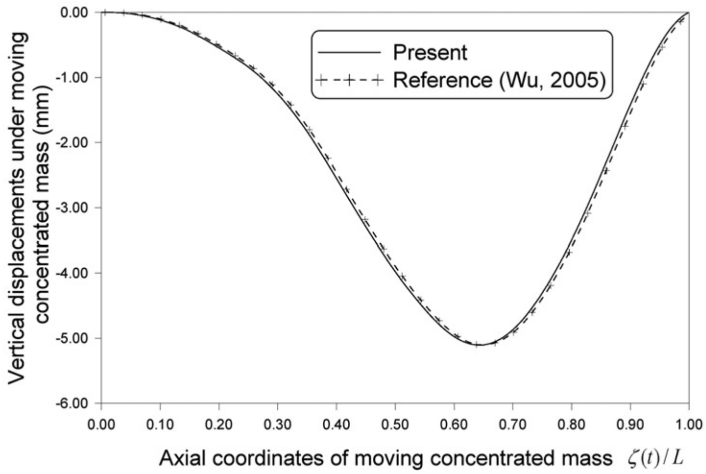

Figure 6. Time histories of vertical displacements under simulated moving concentrated mass.

For $\dot{\bar{\theta}}^*(t)$, the pitch rate of the vehicle at time t is given by

$$\dot{\bar{\theta}}^*(t) = \dot{\bar{\theta}}(t_F) + \ddot{\bar{\theta}}^*(t)(t - t_F). \tag{37}$$

For $\bar{y}^*(t)$, the displacement of the vehicle's center of gravity at time t is given by

$$\bar{y}^*(t) = \sum_{i=1}^{N} \sin\left(\frac{i\pi\zeta}{L}\right) Y_i^*(t) + d_1\bar{\theta}^*(t). \tag{38}$$

For $\dot{\bar{y}}^*(t)$, the velocity of the vehicle's center of gravity at time t is given by

$$\dot{\bar{y}}^*(t) = \sum_{i=1}^{N} \sin\left(\frac{i\pi\zeta}{L}\right) \dot{Y}_i^*(t) + d_1\dot{\bar{\theta}}^*(t). \tag{39}$$

5. Numerical validation and examples

With the results obtained in the previous sections, we selected several values for the number of modes N in order to analyze the tip-off effect. The difference in tip-off analysis results between $N = 10$ and $N = 20$ is less than 0.01 %. We selected $N = 10$ in the whole numerical simulation; three examples are tested and compared with other researchers' studies.

5.1. *Validation case 1*

Figure 6 shows a comparison of the time histories of the vertical displacement of the contact point of the moving mass obtained by Wu (2005) and those obtained in this study. The figure shows that the difference between the results is negligible.

Table 1. Parameters of the vehicle launch system.

EI	$1.2 \times 10^7\,\mathrm{N \cdot m^2}$	d	3.7 m
ρA	$1.5 \times 10^2\,\mathrm{kg/m}$	d_1	2.5 m
ξ	0.03	ζ_R	0.1 m
L	8.0 m	ζ_F	4.2 m
θ_E	0.5 rad	t_b	0.1 s
m	1.6×10^3 kg	$P_{\max}$	7.0×10^4 N
J	$4.7 \times 10^3\,\mathrm{m^4}$	Δt	0.0001 s

Although the technique proposed in this study is meant for the dynamic analysis of an inclined guideway with contact points with a moving vehicle, it can be used for a horizontal beam if the angle of inclination of the guideway is considered to be close to zero. At the same time, the distance between two contact points is considered to be close to zero (1×10^{-15} m) to simulate the single moving mass problem.

5.2. *Validation case 2*

In this case, we assumed the flexural rigidity of the guideway to be $1.2 \times 10^{15}\,\mathrm{N \cdot m^2}$ to simulate a rigid guideway; this value is equal to that of a pseudo-rigid (PR) guideway. The tip-off analysis results obtained by Yao and Zhang (1998) and those obtained in this study were compared using the parameters listed in Table 1. With time, the results obtained using the two approaches deviated slightly.

The numerical results of the analysis are shown in Figures 7 and 8. In fact, the vehicle continues to maintain its uniform rotational acceleration with respect to its rear shoe when the front shoe loses contact with the rigid guideway. As we know, the slope

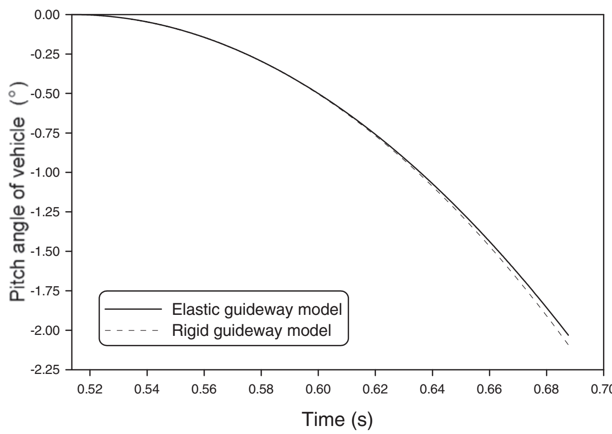

Figure 7. Comparison of pitch angles $\bar{\theta} - t$ of vehicle on PR and rigid guideways.

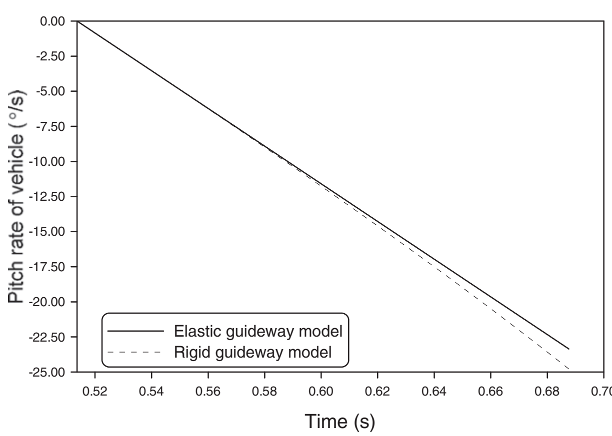

Figure 8. Comparison of pitch rates $\dot{\bar{\theta}} - t$ of vehicle on PR and rigid guideways.

of the pitch rate with respect to time should be almost constant when the motion is a uniform rotational acceleration. A nearly straight line is obtained in our study (Figure 8), as compared to the slightly curved line obtained by Yao and Zhang (1998). Therefore, the analytical technique presented in this study is probably more accurate than that proposed by Yao and Zhang.

5.3. *Test example: behavior of rigid vehicle on elastic guideway*

The parameters of the vehicle launch system used to study the dynamic interaction behavior of a rigid vehicle on an elastic guideway are listed in Table 1. In this test example, we obtained the time interval of the tip-off phase; this started at $t_F = 0.5136$ s and ended at $t_R = 0.6876$ s. Figures 9 and 10 show the time graph of vertical displacement and velocity of vehicle's center of

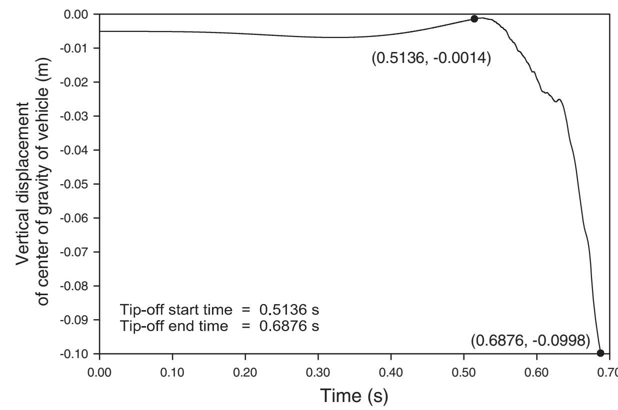

Figure 9. Vertical displacement of vehicle's center of gravity.

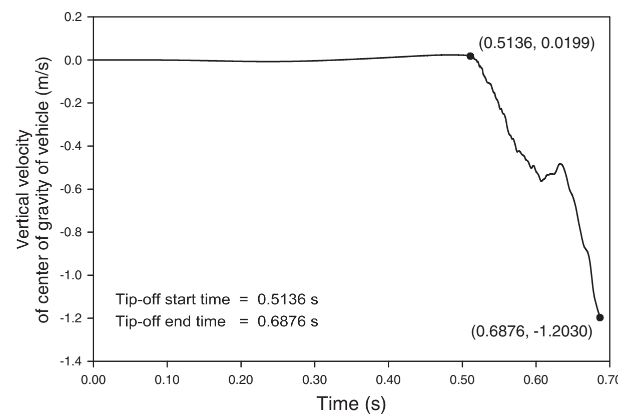

Figure 10. Vertical velocity of vehicle's center of gravity.

gravity, respectively. It shows that the position of the center of gravity of the vehicle tends to move upward before the tip-off phase. The vehicle vibrated excessively violent at approximately 0.6 s during the tip-off phase. Figures 11 and 12 show the comparison of tip-off results of vehicle on elastic and rigid guideways.

According to the parameters listed in Table 1, we estimated the values of parameters such as the damping ratio ξ, angle of inclination θ_E, length of guideway L, and distance between shoes of the vehicle d, and used L and d for the tip-off analysis. Figures 13 and 14 show the typical numerical results of the pitch rate analysis of the vehicle. From the contour lines, we can easily select a set of optimum parameters when designing launch systems.

6. Conclusions

The tip-off effect analysis of a vehicle has been carried out using the modal superposition method by

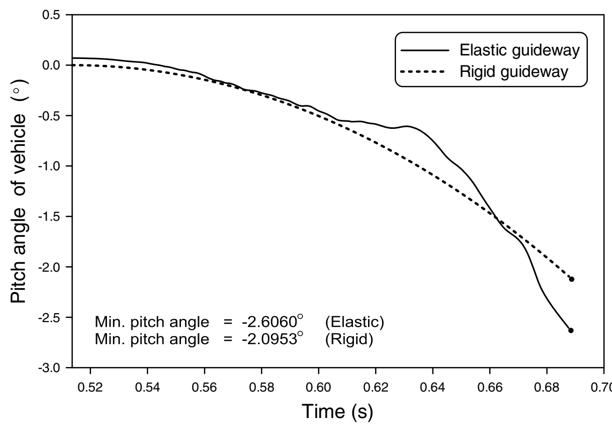

Figure 11. Comparison of pitch angles of vehicle on elastic and rigid guideways.

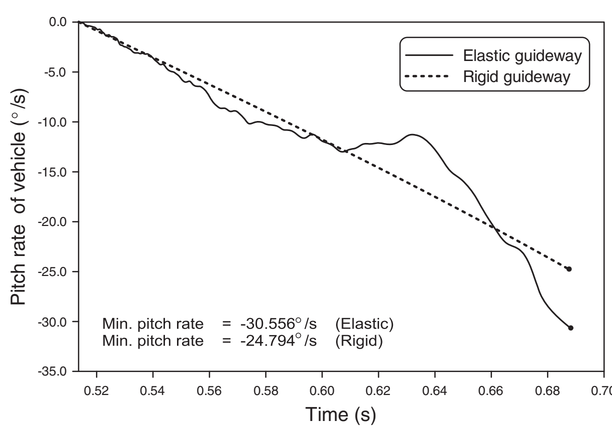

Figure 12. Comparison of pitch rates of vehicle on elastic and rigid guideways.

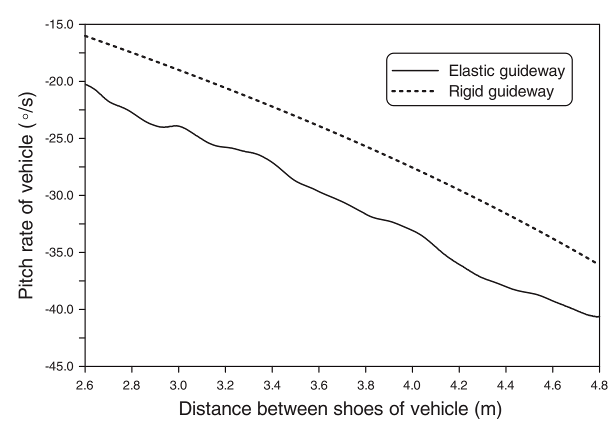

Figure 13. Effect of distance between the shoes of the vehicle on pitch rate of vehicle ($\dot{\bar{\theta}} - d$ diagram).

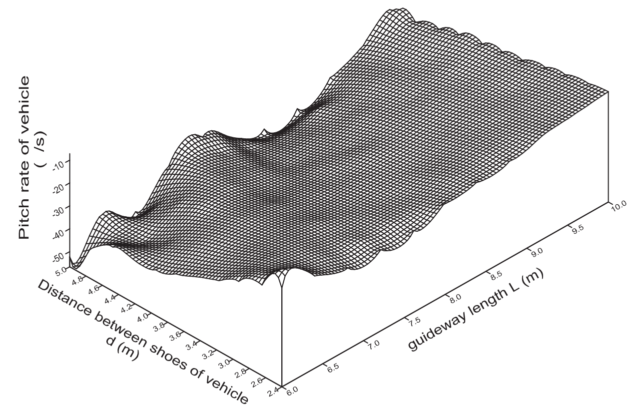

Figure 14. Effect of tip-off analysis on $\dot{\bar{\theta}}_{\max} - L - d$ diagram.

considering the dynamic interaction between a rigid accelerated vehicle and its inclined elastic guideway. The equations obtained in this study are derived by taking into account equations for the influences of the inertia force, Coriolis force, and centrifugal force induced by the vehicle as well as the dynamic interaction between the vehicle and its guideway. From the results obtained in this study, numerical results for the vehicle in the tip-off phase can be easily computed. The following are the conclusions of this study.

(1) The excellent agreement between the previous results and those obtained in this study indicates that the proposed method has been successfully derived.
(2) Generally, the mass of a launched vehicle is considerably larger than that of its guideway. In this case, the problem of moving loads can be solved by an analysis of the dynamic response of a light beam under the action of a heavy moving load. This analysis differs from that of the vehicle–bridge interaction dynamics in civil engineering. If the rigid guideway model is adopted to calculate the tip-off effect of a vehicle in the take-off phase, it may lead to incorrect results because this model does not consider the dynamic interaction between the vehicle and its guideway.
(3) A comparison of the tip-off analysis results for the elastic and rigid guideway models in a test example shows that the dynamic response obtained for the elastic guideway model was 20 % greater than that obtained for the rigid guideway model. This highlights the importance of adopting the elastic guideway model when designing actual launch systems.

(4) The movement of a vehicle along a guideway has complex effects on the launcher, and these effects may increase when the vehicle fires before its take-off. Thrust asymmetry and manufacturing defects tend to make the vehicle rotate, pitch, or yaw. The guideway restrains these motions. Therefore, a more rigorous analysis of the dynamic interactions is required.

Nomenclature

$P(t)$	thrust force acting on vehicle
θ_E	angle of inclination of guideway
EI	flexural rigidity of guideway
L	length of guideway
ξ	damping ratio of guideway
ρA	mass per unit length of guideway
m	mass of vehicle
J	mass moment of inertia of vehicle
d	distance between shoes of vehicle
d_1	distance between rear shoe and center of gravity of vehicle
$F(t)$	front shoe contact forces between vehicle and guideway
$R(t)$	rear shoe contact forces between vehicle and guideway
$\zeta(t)$	position coordinate of vehicle on guideway
$\dot{\zeta}(t)$	velocity of vehicle on guideway
$\ddot{\zeta}(t)$	acceleration of vehicle on guideway
ζ_R	distance from rear shoe of vehicle to left end of guideway at $t=0$
ζ_F	distance from front shoe of vehicle to right end of guideway at $t=0$
t_b	time of thrust build-up
t_F	time at which front shoe of vehicle loses contact
t_R	time at which vehicle takes-off

References

Dehestani, M., Mofid, M., and Vafai, A., 2009. Investigation of critical influential speed for moving mass problems on beams. *Applied mathematical modelling*, 33 (10), 3885–3895.

Fryba, L., 1999. *Vibration of solids and structures under moving loads*. 3rd ed. London: Thomas Telford.

Lin, J.H. and Weng, C.C., 2004. Evaluation of dynamic vehicle load on bridge decks. *Journal of the Chinese institute of engineers*, 27 (5), 695–705.

Michaltsos, G.T., 2002. Dynamic behaviour of a single-span beam subjected to loads moving with variable speeds. *Journal of sound and vibration*, 258 (2), 359–372.

Michaltsos, G., Sophianopoulos, D., and Kounadis, A.N., 1996. The effect of a moving mass and other parameters on the dynamic response of a simply supported beam. *Journal of sound and vibration*, 191 (3), 357–362.

Wu, J.J., 2005. Dynamic analysis of an inclined beam due to moving loads. *Journal of sound and vibration*, 288 (1–2), 107–131.

Xia, H. and Zhang, N., 2005. *Dynamic interaction of vehicles and structures*. Beijing: Science Press.

Xia, H., Zhang, N., and Roeck, G.D., 2003. Dynamic analysis of high speed railway bridge under articulated trains. *Computers and structures*, 81 (26–27), 2467–2478.

Yang, Y.B. and Wu, Y.S., 2005. Transmission of vibrations from high speed trains through viaducts and foundations to the ground. *Journal of the Chinese institute of engineers*, 28 (2), 251–266.

Yang, Y.B., Yau, J.D., and Hsu, L.C., 1997. Vibration of simple beams due to trains moving at high speeds. *Engineering structures*, 19 (11), 936–944.

Yao, C.R. and Zhang, P., 1998. *Rocket and guided missile launcher device design*. Beijing: Beijing Institute of Technology Press.